Erratum: Coupling effects in proton scattering from ^{40}Ca

Journal Item

Erratum: Coupling effects in proton scattering from ^{40}Ca [Phys. Rev. C 85, 064603 (2012)]

R. S. Mackintosh and N. Keeley

(Received 21 February 2018; published 1 June 2018)

DOI: 10.1103/PhysRevC.97.069901

Since the publication of our article it has come to our attention that, due to a bug in the version of FRESCO [1] employed, some of the calculations presented in the original paper are incorrect. (FRESCO was corrected for Version 2.93 of May-August 2012.) The calculations affected are those labeled "All ($3 \times 5/2^+$)," "All ($9 \times 5/2^+$)," and "Linearity test" in Table I and "All ($3 \times 5/2^+$) UD" (where UD represents up-down) in Table IV. We give here corrected versions of Figs. 1–3 and Tables I and IV.

It will be seen that the dynamic polarization potential for the full cases is now greater in magnitude with some terms changed in sign. The version of FRESCO used produced erroneous results when two circumstances hold: (i) Two or more states with the same spin parity are coupled to the elastic channel, and (ii) the deuteron potential is calculated by FRESCO using the Watanabe folding model. The new results using the updated FRESCO exhibit a real dynamic polarization potential (DPP) having a very

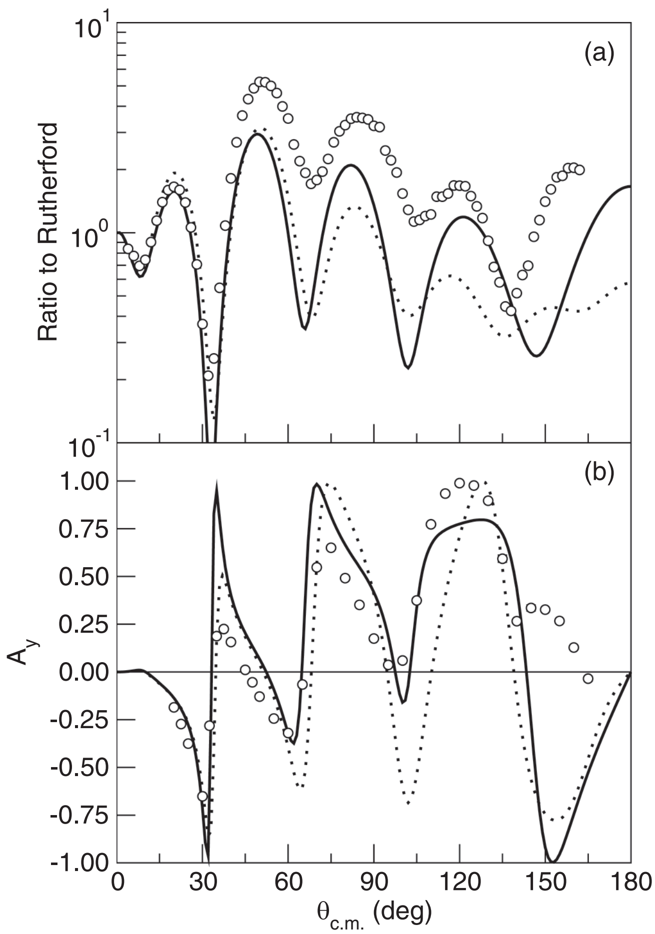

FIG. 1. For 30.3 MeV protons scattering from ^{40}Ca, the (a) angular distribution (AD) and (b) analyzing power (AP) for the case of All ($3 \times 5/2^+$) in Table I compared with the measured values. The dotted line presents UD calculations for the same case as described in Sec. III D.

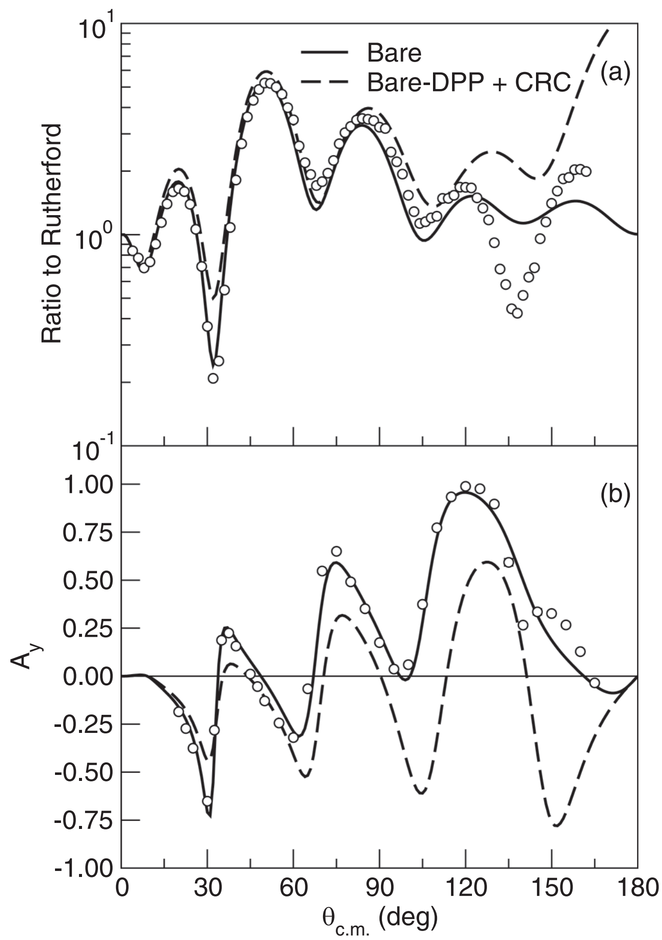

FIG. 2. For 30.3 MeV protons scattering from ^{40}Ca, the (a) AD and (b) AP for the All ($3 \times 5/2^+$) coupled reaction channel (CRC) calculation involving a modified bare potential in which the DPP has been subtracted from the original bare potential of Ref. [15], compared with a no-coupling calculation using the bare potential of Ref. [15].

TABLE I. For protons scattering from ^{40}Ca at 30.3 MeV/nucleon, volume integrals ΔJ (in MeV fm^3) of the four components of the DPP induced by (p,d) coupling. The $\Delta R_{\rm rms}$ column gives the change in rms radius of the real central component (in femtometers). The two final columns, respectively, present the change in the total reaction cross section (CS) induced by the coupling and the integrated cross section to the specific coupled reaction channels. Note that negative $\Delta J_{\rm R}$ corresponds to repulsion. The excitation energies of the states in MeV are given in parentheses.

States coupled	$\Delta J_{\rm R}$	$\Delta J_{\rm IM}$	$\Delta J_{\rm RSO}$	$\Delta J_{\rm IMSO}$	$\Delta R_{\rm rms}$	Δ(Reaction CS) (mb)	State CS (mb)
$3/2^+$ (0.0)	−12.53	14.64	0.8605	−0.3257	0.0344	52.47	7.93
$1/2^+$ (2.467)	−4.00	5.62	0.2224	0.0894	0.0088	25.77	6.51
$5/2^+$ (5.6175)	−3.36	10.35	0.5100	0.3339	0.0206	39.26	4.95
$5/2^+$ (7.3148)	−0.75	3.58	0.1918	0.0964	0.0071	15.33	1.61
$5/2^+$ (8.5148)	−0.4	2.99	0.1697	0.0712	0.0058	13.26	1.15
$7/2^-$ (2.796)	+0.42	1.29	0.118	0.0083	0.0018	6.3	0.889
Sum (of above)	−20.62	38.47	2.0724	0.2735	0.0785	152.39	23.0
All ($3 \times 5/2^+$)	−7.77	59.74	3.708	−1.719	0.0332	147.03	15.1
All ($9 \times 5/2^+$)	−7.47	59.69	3.707	−1.71	0.0332	146.93	15.1
Linearity test	−3.92	−13.49	−1.906	1.132	0.0108	−112.41	44.7

different form at small radii. This can be attributed to coupling to the second $\frac{5}{2}^+$ state at 7.3148 MeV. Figure 4 shows this: The difference between the dotted line and the dot-dashed line is that the former represents the DPP when the second $\frac{5}{2}^+$ state at 7.3148 MeV is included. In this figure the solid line presents the DPP for coupling to the $\frac{3}{2}^+$ ground state and the $\frac{1}{2}^+$ state at 2.467 MeV. The dashed line represents the additional coupling to the $\frac{7}{2}^-$ state at 2.796 MeV; the dashed-dotted line includes the $\frac{5}{2}^+$ state at 5.6175 MeV; the dotted lines show the effect of the second $\frac{5}{2}^+$ state and suggest the large change resulting from the full complement of $\frac{5}{2}^+$ states leading to the DPP shown in Fig. 3. Further work is in progress to throw light on the conditions under which this remarkable phenomenon occurs.

TABLE IV. For protons scattering from ^{40}Ca at 30.3 MeV/nucleon, volume integrals ΔJ (in MeV fm^3) of the four components of the DPP induced by (p,d) coupling. The $\Delta R_{\rm rms}$ column gives the change in rms radius of the real-central component (in femtometers). The two final columns, respectively, present the change in the total reaction cross section induced by the coupling and the integrated cross section to the specific coupled reaction channels. Note that negative $\Delta J_{\rm R}$ corresponds to repulsion. The line numbers are referred to in the text.

States coupled	$\Delta J_{\rm R}$	$\Delta J_{\rm IM}$	$\Delta J_{\rm RSO}$	$\Delta J_{\rm IMSO}$	$\Delta R_{\rm rms}$	Δ(Reaction CS) (mb)	State CS (mb)	Line
$3/2^+$	−12.53	14.64	0.8605	−0.3257	0.0344	52.47	7.93	1
$3/2^+$ UD	−12.82	11.97	0.6509	−0.0324	0.0314	41.35	8.0542	2
$3/2^+$ UD, sum rule	−23.89	19.69	1.1855	0.1145	0.0522	60.67	13.486	3
$3/2^+$ UD, ×1.6744	−21.47	20.04	1.0899	−0.0543	0.0526	69.24	13.486	4
$3/2^+$ sum rule	−23.66	30.55	2.1445	−1.6233	0.0675	94.27	12.88	5
$3/2^+$ ×1.6744	−20.98	24.51	1.4408	−0.5454	0.0576	87.86	13.28	6
$1/2^+$	−4.00	5.62	0.2224	0.0894	0.0088	25.77	6.51	7
$1/2^+$ UD	−4.11	5.24	0.2080	0.0935	0.0083	23.92	6.6234	8
$1/2^+$ UD, sum rule	−11.6	12.86	0.5013	0.2887	0.0212	53.05	16.332	9
$1/2^+$ UD ×2.4658	−10.13	12.92	0.5130	0.2306	0.0205	58.98	16.332	10
$1/2^+$ sum rule	−11.19	15.55	0.6270	0.2718	0.0231	64.54	15.376	11
$1/2^+$ ×2.4658	−9.86	13.86	0.5484	0.2204	0.0217	63.54	16.05	12
All ($3 \times 5/2^+$) UD	−30.52	36.24	1.985	1.464	0.105	99.03	23.61	13

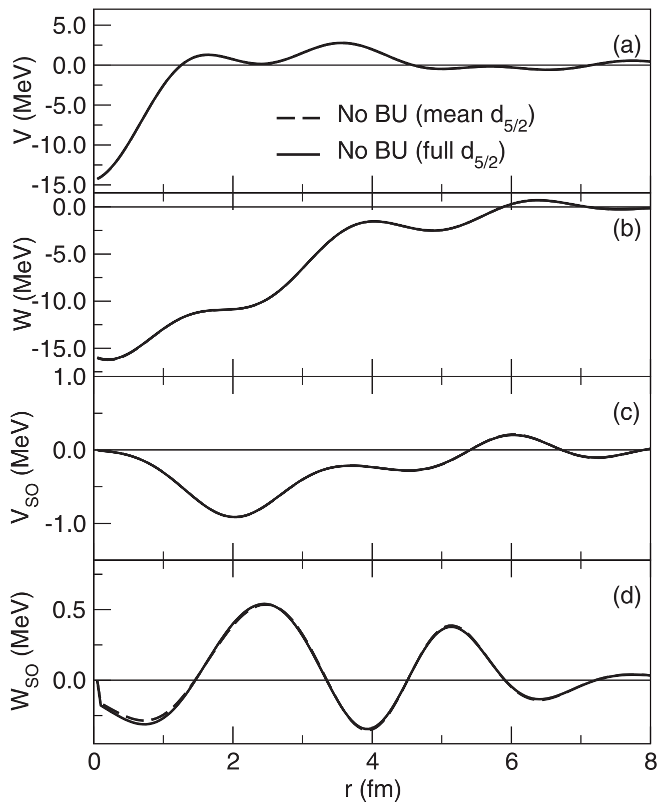

FIG. 3. For 30.3 MeV protons scattering from ^{40}Ca, the DPPs calculated by inversion and subtraction of the bare potential. The dashed lines are for the case of All ($3 \times 5/2^+$), and the solid lines for the All ($9 \times 5/2^+$) case. From top to bottom, we present the (a) real and (b) imaginary central DPPs, then the (c) real and (d) imaginary spin-orbit DPPs. Note that the solid and dashed curves are now graphically indistinguishable.

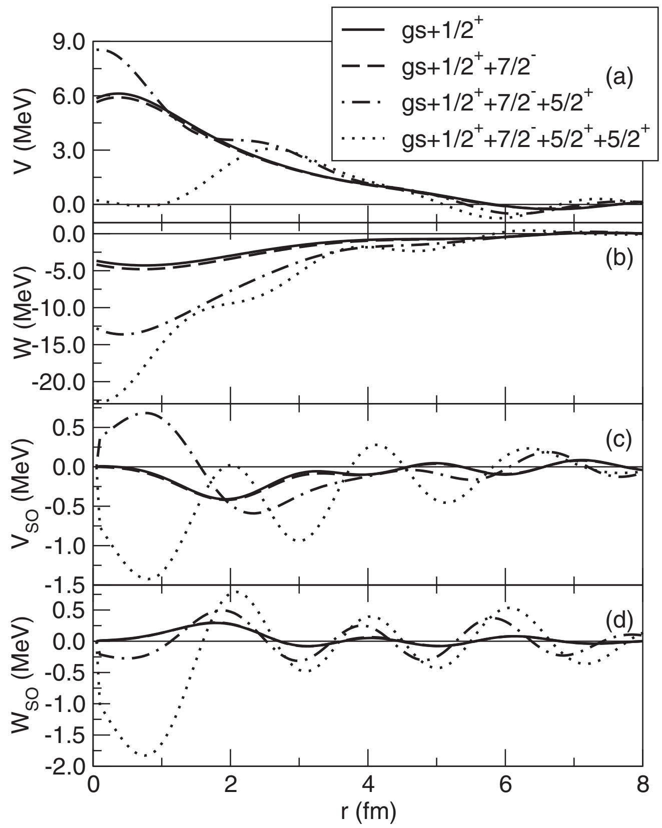

FIG. 4. For 30.3 MeV protons scattering from ^{40}Ca, the DPPs calculated by inversion and subtraction of the bare potential. The lines are identified in the text. From top to bottom, we present the (a) real and (b) imaginary central DPPs, then the (c) real and (d) imaginary spin-orbit DPPs.

[1] I. J. Thompson, Comput. Phys. Rep. **7**, 167 (1988).
[15] V. Hnizdo, O. Karban, J. Lowe, G. W. Greenlees, and W. Makofske, Phys. Rev. C, **3**, 1560 (1971).